Lithium Insertion and XPS Study in $La_{0.5+x+y}Li_{0.5-3x}Ti_{1-3y}Cr_{3y}O_3$

María-Luisa Martínez-Sarrión,*[a] Lourdes Mestres,[a] Rosa Palacín,[b] and Marta Herráiz[a]

Keywords: Lithium / Insertions / Electrochemistry / Photoelectron spectroscopy

The stoichiometry and lithium insertion reactions with *n*BuLi and by electrochemical techniques of solid solutions $La_{0.5+x+y}Li_{0.5-3x}Ti_{1-3y}Cr_{3y}O_3$ with a perovskite-type structure have been studied. Stoichiometry data are given in the form of a solid solution triangle. In general, the amount of lithium inserted is consistent with the number of vacancies. The results of the chemical and electrochemical lithium insertion are similar: upon lithium insertion Cr^{VI} is reduced to Cr^{III}.

Introduction

Materials with structures derived from the high temperature phase γ-Li_3PO_4 comprise an extensive family of lithium-ion-conducting solid electrolytes known as LISICONS or γ-structures. Recently, a new group of lithium-ion conductors and mixed conductors in the LISICON family have been found that contain $Cr^{[5+]}$ as a framework cation.[1,2] The electrochemical intercalation of lithium into chromium(V)-containing oxides isostructural with β- and γ-Li_3PO_4 has been studied. β-Li_3CrO_4 can reversibly intercalate around one mol of Li per formula unit to give $Li_{3+x}CrO_4$ ($0 < x < 1$) with a discharge capacity of 196 $mAhg^{-1}$. Electrochemical data indicate that there may be a region with two phases in the approximate range $0.3 < x < 0.8$. Essentially, these materials are dimensionally stable to intercalation and de-intercalation.[3]

The X-ray photoelectron spectra of the different compounds of Cr^{III} were measured and from these data the chemical shifts of the core electrons were determined and related to a calculated charge based on Pauling's electronegativities.[4] A few years ago the binding energies of the chromium(III) 2p electrons was proposed to be dependent primarily on the oxidation number, although perturbations result from changes in the structure and in the Madelung potential. Multiplet splitting in chromium(III) compounds contributes to peak widths and the chemisorption of water and oxygen has a marked effect on the peak profiles and the accuracy of binding energy measurements.[5]

The electronic structures of the perovskite system $La_{1-x}(M^{2+})_xCrO_3$ (M = Mg, Sr) has been more widely studied than Cr_2O_3 and La_2O_3 by X-ray photoelectron spectroscopy. The main peaks and satellites of inner and outer electrons were properly assigned.[6]

Spinel solid solutions of general formula $ZnCr_xGa_{2-x}O_4$ have been studied by X-ray photoelectron spectroscopy. These XPS spectra indicated that in the spinel solid solutions no significant change in the electronic structure of Cr^{3+} ions occur, and a similar covalency in all the $ZnCr_xGa_{2-x}O_4$ solid solutions, irrespective of their composition, has been reported.[7]

In a previous paper[8] we studied the $La_{0.5+x+y}Li_{0.5-3x}Ti_{1-3y}Mn_{3y}O_3$ system, and the bulk conductivity data from the impedance complex plane plots were plotted in an Arrhenius format. The plots are linear and the conductivity decreases as the amount of lithium decreases. The variation in ionic conductivity with the lithium composition is quite large, although the ionic and electronic conductivity remain similar for $y = 0.01$.

The $Pr_{0.5+x+y}Li_{0.5-3x}Ti_{1-3y}Cr_{3y}O_3$ system showed similar behavior.[9] AC/DC measurements indicated that these compounds are mixed conductors. The Li^+ conductivity decreases as the amount of lithium decreases, while electronic conductivity increases with the amount of chromium. Similar measurements indicate that $La_{0.5+x+y}Li_{0.5-3x}Ti_{1-3y}Cr_{3y}O_3$ compounds are mixed conductors. The lithium ion conductivity decreases as the amount of lithium decreases, meanwhile electronic conductivity increases with the amount of chromium.[10]

Here we examine the chemical and electrochemical insertion and de-insertion of lithium in $La_{0.5+x+y}Li_{0.5-3x}Ti_{1-3y}Cr_{3y}O_3$ mixed conductors.

Results and Discussion

Chemical lithium intercalation was carried out on different compositions of the region of perovskite-like solid solutions on the phase diagram.[10] Along join 1 ($La_{0.583}Li_{0.25}TiO_3-LaCrO_3$), the lithium and lanthanum composition and the number of vacancies changes, along join 2 ($La_{0.60}Li_{0.20}TiO_3-La_{0.80}Li_{0.20}Ti_{0.40}Cr_{0.60}O_3$) the amount of lithium was constant, along join 3 ($La_{0.567}Li_{0.30}TiO_3-La_{0.86}Ti_{0.40}Cr_{0.60}O_3$), the number of vacancies was constant, along join 4 ($La_{0.583}Li_{0.25}TiO_3-La_{0.75}Li_{0.25}Ti_{0.50}Cr_{0.50}O_3$), the amount of lithium was constant, and along join 5

[a] Departament de Química Inorgànica, Universitat de Barcelona, Diagonal 647, 08028 Barcelona, Spain,
Fax: (internat.) +34-93/490-7725
E-mail: marialuisa.martinez@qi.ub.es
[b] Institut de Ciència de Materials de Barcelona (C.S.I.C.), Campus U.A.B., 08193 Bellaterra, Spain

  1434−1948/01/0505−1139 $ 17.50+.50/0

($La_{0.86}Ti_{0.40}Cr_{0.60}O_3-La_{0.80}Li_{0.20}Ti_{0.40}Cr_{0.60}O_3$) the chromium amount was constant (Figure 1).

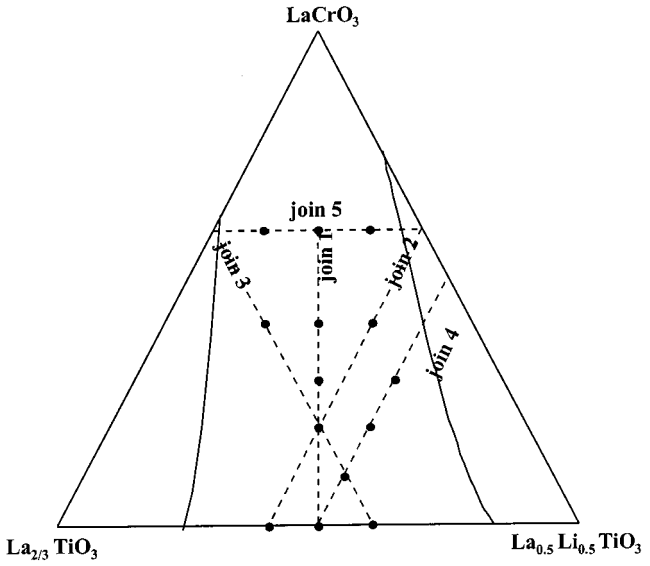

Figure 1. Composition triangle and joins of chemical lithium intercalation

ICP analyses were then carried out and these results are shown in Table 1, with the (Cr + Ti) amount set to unity and the remaining values re-normalised in the formula $La_{0.5+x+y}Li_{0.5-3x}Ti_{1-3y}Cr_{3y}O_3$. In general, the amount of lithium inserted is consistent with the number of vacancies. For all compositions the Li:La:Ti:Cr ratios were in good agreement with the values expected from the starting compositions.

The compositions along join 1 were measured by EPMA. The experimental values of oxygen contents have larger uncertainties than the values for La, Ti and Cr due to the difficulty in separating the O-K_α signal from that emitted by the carbon coating and partial absorption of the O-K_α signal by the carbon. $SrTiO_3$, which was the standard for oxygen, and some samples were coated together to improve the oxygen measurements. The results obtained in join 1,[10] allowed us to establish that the oxygen content varies between 2.95 and 3.01. For this reason we assume that the oxygen content in all the samples is nearly to 3.

Figures 2–5 show the amount of lithium inserted versus amount of lanthanum for joins 1, 3, 4 and 5, respectively. In join 1 (where the lithium and lanthanum composition and the number of vacancies changes), when the lanthanum and chromium amount increases, the number of vacancies decreases, therefore the amount of lithium inserted must also decrease. In Figure 2 we can see this behavior, except for the sample $La_{0.71}Li_{0.19}Ti_{0.69}Cr_{0.31}O_3$ in which 0.16 mol of lithium is inserted. This behaviour can be attributed to the cubic structure of the $La_{0.58}Li_{0.25}TiO_3$ and $La_{0.70}Li_{0.21}Ti_{0.79}Cr_{0.21}O_3$ compounds and the orthorhombic structure of $La_{0.71}Li_{0.19}Ti_{0.69}Cr_{0.31}O_3$, $La_{0.76}Li_{0.17}Ti_{0.59}Cr_{0.41}O_3$, and $La_{0.83}Li_{0.07}Ti_{0.39}Cr_{0.61}O_3$.[10] In join 3 (the number of vacancies was constant), the substitution of chromium for titanium increases the amount of lithium inserted, which decreases with an increase in the amount of lanthanum. In join 4 (the lithium amount was constant), when lanthanum and chromium increase, the number of vacancies decreases, and, consequently, the amount of lithium inserted is reduced. In join 5 (the chromium amount was constant) the lithium insertion increases as the number of vacancies increases.

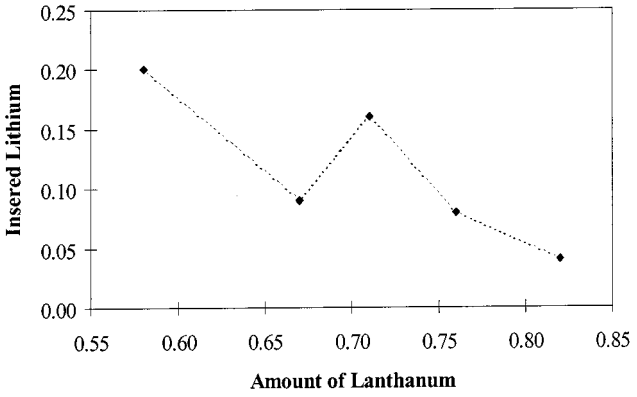

Figure 2. Plot of amount of lithium inserted vs. amount of lanthanum in join 1

Table 1. Samples composition and vacancies before and after the insertion of lithium

Starting composition $La_{0.5+x+y}Li_{0.5-3x}Ti_{1-3y}Cr_{3y}O_3$	Experimental composition	Inserted Lithium $La_{0.5+x+y}Li_{0.5-3x+\delta}Ti_{1-3y}Cr_{3y}O_3$	A-site vacancy[a]	δ
$La_{0.60}Li_{0.20}TiO_3$	$La_{0.62}Li_{0.18}TiO_3$	$La_{0.62}Li_{0.39}TiO_3$	0.20	0.21
$La_{0.58}Li_{0.25}TiO_3$	$La_{0.58}Li_{0.25}TiO_3$	$La_{0.58}Li_{0.45}TiO_3$	0.17	0.20
$La_{0.57}Li_{0.30}TiO_3$	$La_{0.57}Li_{0.27}TiO_3$	$La_{0.57}Li_{0.45}TiO_3$	0.16	0.18
$La_{0.62}Li_{0.25}Ti_{0.90}Cr_{0.10}O_3$	$La_{0.64}Li_{0.22}Ti_{0.89}Cr_{0.11}O_3$	$La_{0.64}Li_{0.34}Ti_{0.90}Cr_{0.10}O_3$	0.14	0.12
$La_{0.67}Li_{0.20}Ti_{0.80}Cr_{0.20}O_3$	$La_{0.70}Li_{0.21}Ti_{0.79}Cr_{0.21}O_3$	$La_{0.70}Li_{0.30}Ti_{0.79}Cr_{0.21}O_3$	0.09	0.09
$La_{0.65}Li_{0.25}Ti_{0.80}Cr_{0.20}O_3$	$La_{0.67}Li_{0.24}Ti_{0.79}Cr_{0.21}O_3$	$La_{0.67}Li_{0.33}Ti_{0.79}Cr_{0.21}O_3$	0.09	0.09
$La_{0.71}Li_{0.175}Ti_{0.70}Cr_{0.30}O_3$	$La_{0.70}Li_{0.17}Ti_{0.69}Cr_{0.31}O_3$	$La_{0.70}Li_{0.33}Ti_{0.69}Cr_{0.31}O_3$	0.10	0.16
$La_{0.68}Li_{0.25}Ti_{0.70}Cr_{0.30}O_3$	$La_{0.69}Li_{0.24}Ti_{0.69}Cr_{0.31}O_3$	$La_{0.69}Li_{0.32}Ti_{0.69}Cr_{0.31}O_3$	0.07	0.08
$La_{0.77}Li_{0.10}Ti_{0.60}Cr_{0.40}O_3$	$La_{0.80}Li_{0.08}Ti_{0.55}Cr_{0.45}O_3$	$La_{0.80}Li_{0.15}Ti_{0.56}Cr_{0.44}O_3$	0.12	0.07
$La_{0.75}Li_{0.15}Ti_{0.60}Cr_{0.40}O_3$	$La_{0.76}Li_{0.17}Ti_{0.59}Cr_{0.41}O_3$	$La_{0.76}Li_{0.25}Ti_{0.59}Cr_{0.41}O_3$	0.07	0.08
$La_{0.73}Li_{0.20}Ti_{0.60}Cr_{0.40}O_3$	$La_{0.71}Li_{0.20}Ti_{0.59}Cr_{0.41}O_3$	$La_{0.71}Li_{0.28}Ti_{0.59}Cr_{0.41}O_3$	0.09	0.08
$La_{0.85}Li_{0.05}Ti_{0.40}Cr_{0.60}O_3$	$La_{0.84}Li_{0.04}Ti_{0.39}Cr_{0.61}O_3$	$La_{0.84}Li_{0.09}Ti_{0.39}Cr_{0.61}O_3$	0.12	0.05
$La_{0.83}Li_{0.10}Ti_{0.40}Cr_{0.60}O_3$	$La_{0.82}Li_{0.07}Ti_{0.39}Cr_{0.61}O_3$	$La_{0.82}Li_{0.11}Ti_{0.39}Cr_{0.61}O_3$	0.11	0.04
$La_{0.82}Li_{0.15}Ti_{0.40}Cr_{0.60}O_3$	$La_{0.80}Li_{0.13}Ti_{0.39}Cr_{0.61}O_3$	$La_{0.80}Li_{0.15}Ti_{0.39}Cr_{0.61}O_3$	0.07	0.02

[a] (calculated A-site vacancy) = 1 − (La content + Li content).

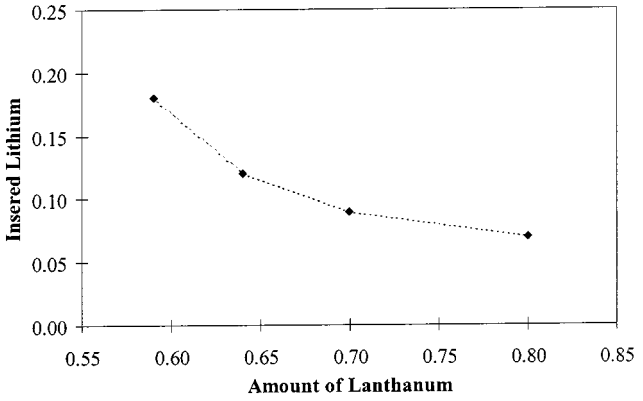

Figure 3. Plot of amount of lithium inserted vs. amount of lanthanum in join 3

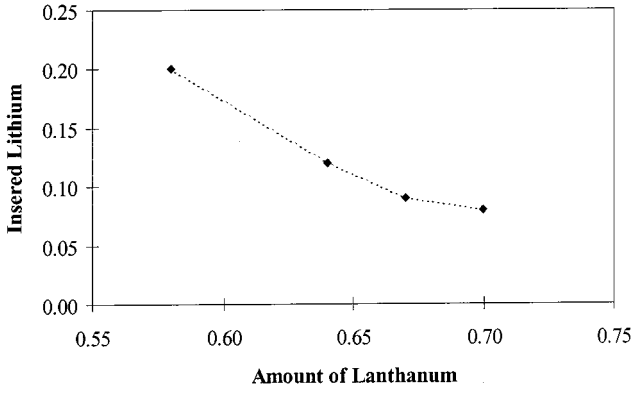

Figure 4. Plot of amount of lithium inserted vs. amount of lanthanum in join 4

The cell parameters of the lithium inserted phases show no differences with the non-lithium inserted phases (Table 2).

De-lithiation reactions were performed by treating some compositions of the lithiated compounds with iodine in dry acetonitrile. The results are shown in Table 3. The process of lithium insertion-delithiation is reversible.

The degrees of lithium uptake observed in electrochemical experiments down to 1.5 V vs. Li^0-Li^+ were approximately consistent with those obtained after chemical lithiation. Some typical composition-voltage profiles are shown in Figure 6, corresponding to samples along join 4 containing both titanium and chromium. Contrary to what has been reported for pure La−Li−Ti−O perovskites,[11,12] the degree of lithium intercalation in chromium-containing samples is never higher, within the experimental errors, than the number of A-type vacancies. On the other hand, the increase in the chromium content seems to be associated with an electrochemical step appearing at about 2.3 V vs. Li^0-Li^+ upon reduction of the samples. The electrochemical de-intercalation (i.e. oxidation) is difficult to achieve and only takes place at ≈4V, (Figure 6) for sample $La_{0.69}Li_{0.24}Ti_{0.69}Cr_{0.31}O_3$.

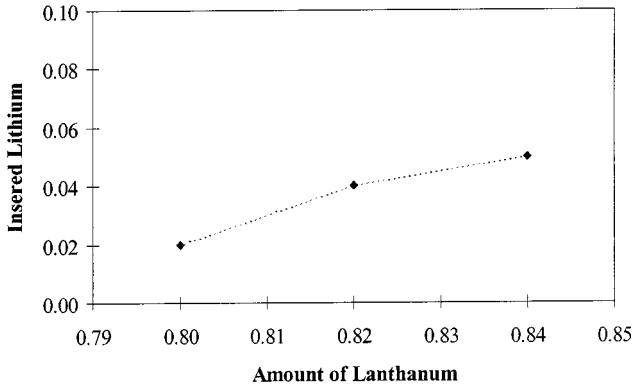

Figure 5. Plot of amount of lithium inserted vs. amount of lanthanum in join 5

The X-ray photoelectron spectroscopy of different compositions were compared with the values from Table 4. Figure 7 shows the Cr (2p) spectrum for the composition $La_{0.92}Li_{0.05}Ti_{0.21}Cr_{0.79}O_3$ (c in Figure 7), and we compared this with the patterns of Cr_2O_3 (a) and CrO_3 (b) from 565 to 605 eV. The main peaks of this sample, located at 576.2 eV ($Cr2p_{3/2}$) and 585.9 eV ($Cr2p_{1/2}$), correspond to Cr^{3+}. The shake-up satellite of $Cr2p_{3/2}$ is seen at ≈582 eV and, for $Cr(2p_{1/2})$, the satellite appears at ≈597 eV. The main peaks of chromium show a shoulder that indicates the presence of chromium in another number state, probably Cr^{6+} (Fig-

Table 2. Cell parameters of the samples before and after the insertion of lithium

Starting sample	Inserted sample	*a* (A)	*b* (A)	*c* (A)	*V* (A^3)
$La_{0.64}Li_{0.22}Ti_{0.89}Cr_{0.11}O_3$		3.8775(6)	3.8775(6)	3.8775(6)	58.298(2)
	$La_{0.64}Li_{0.34}Ti_{0.90}Cr_{0.10}O_3$	3.8775(6)	3.8775(6)	3.8775(6)	58.298(2)
$La_{0.70}Li_{0.21}Ti_{0.79}Cr_{0.21}O_3$		3.8768(6)	3.8768(6)	3.8768(6)	58.266(2)
	$La_{0.70}Li_{0.30}Ti_{0.79}Cr_{0.21}O_3$	3.8767(6)	3.8767(6)	3.8767(6)	58.262(2)
$La_{0.67}Li_{0.24}Ti_{0.79}Cr_{0.21}O_3$		3.8765(7)	3.6765(7)	3.8765(7)	58.25(2)
	$La_{0.67}Li_{0.33}Ti_{0.79}Cr_{0.21}O_3$	3.8767(6)	3.8767(6)	3.8767(6)	58.267(2)
$La_{0.70}Li_{0.17}Ti_{0.69}Cr_{0.31}O_3$		5.491(9)	5.481(3)	7.757(9)	233.46(2)
	$La_{0.70}Li_{0.33}Ti_{0.69}Cr_{0.31}O_3$	5.491(6)	5.479(6)	7.754(7)	233.28(2)
$La_{0.69}Li_{0.24}Ti_{0.69}Cr_{0.31}O_3$		3.8765(7)	3.8765(7)	3.8765(7)	58.25(2)
	$La_{0.69}Li_{0.32}Ti_{0.69}Cr_{0.31}O_3$	3.8767(3)	3.8767(3)	3.8767(3)	58.262(1)
$La_{0.80}Li_{0.08}Ti_{0.55}Cr_{0.45}O_3$		5.497(7)	5.480(5)	7.759(8)	233.73(2)
	$La_{0.80}Li_{0.15}Ti_{0.56}Cr_{0.44}O_3$	5.495(6)	5.479(6)	7.762(9)	233.69(2)
$La_{0.76}Li_{0.17}Ti_{0.59}Cr_{0.41}O_3$		5.493(8)	5.480(4)	7.756(8)	233.47(2)
	$La_{0.76}Li_{0.25}Ti_{0.59}Cr_{0.41}O_3$	5.493(9)	5.480(6)	7.756(9)	233.47(2)
$La_{0.82}Li_{0.07}Ti_{0.39}Cr_{0.61}O_3$		5.499(6)	5.479(6)	7.761(9)	233.83(2)
	$La_{0.82}Li_{0.11}Ti_{0.39}Cr_{0.61}O_3$	5.500(7)	5.480(5)	7.763(8)	233.98(2)

Table 3. Sample compositions after chemical lithium removal

Starting composition	Inserted composition	Deintercalation composition
$La_{0.64}Li_{0.22}Ti_{0.89}Cr_{0.11}O_3$	$La_{0.64}Li_{0.34}Ti_{0.90}Cr_{0.10}O_3$	$La_{0.65}Li_{0.21}Ti_{0.90}Cr_{0.10}O_3$
$La_{0.67}Li_{0.24}Ti_{0.79}Cr_{0.21}O_3$	$La_{0.67}Li_{0.33}Ti_{0.79}Cr_{0.21}O_3$	$La_{0.65}Li_{0.22}Ti_{0.79}Cr_{0.21}O_3$
$La_{0.70}Li_{0.17}Ti_{0.69}Cr_{0.31}O_3$	$La_{0.70}Li_{0.33}Ti_{0.69}Cr_{0.31}O_3$	$La_{0.71}Li_{0.16}Ti_{0.61}Cr_{0.39}O_3$
$La_{0.69}Li_{0.24}Ti_{0.69}Cr_{0.31}O_3$	$La_{0.69}Li_{0.32}Ti_{0.69}Cr_{0.31}O_3$	$La_{0.70}Li_{0.23}Ti_{0.69}Cr_{0.31}O_3$
$La_{0.80}Li_{0.08}Ti_{0.55}Cr_{0.45}O_3$	$La_{0.80}Li_{0.15}Ti_{0.56}Cr_{0.44}O_3$	$La_{0.80}Li_{0.10}Ti_{0.57}Cr_{0.43}O_3$
$La_{0.84}Li_{0.04}Ti_{0.39}Cr_{0.61}O_3$	$La_{0.84}Li_{0.09}Ti_{0.39}Cr_{0.61}O_3$	$La_{0.84}Li_{0.06}Ti_{0.63}Cr_{0.37}O_3$
$La_{0.80}Li_{0.13}Ti_{0.39}Cr_{0.61}O_3$	$La_{0.80}Li_{0.15}Ti_{0.39}Cr_{0.61}O_3$	$La_{0.79}Li_{0.10}Ti_{0.39}Cr_{0.61}O_3$

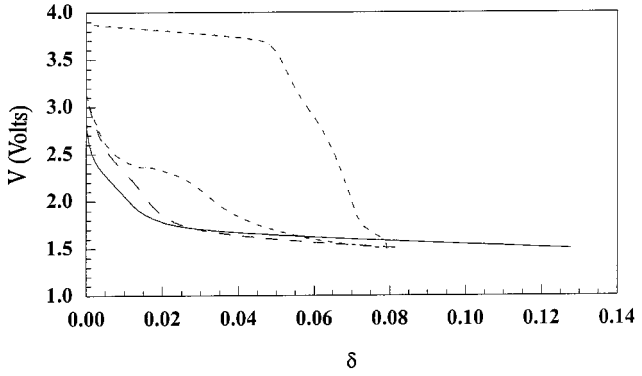

Figure 6. Discharge-charge curves operating in galvanostatic low current mode at 1MLi/200 h

Table 4. Binding energy (eV) observed from the photoelectron spectra for elements in various chromium and titanium compounds

Pattern	Cr 2p 1/2	Cr 2p 3/2	Ti 2p 1/2	Ti 2p 3/2	Ref.
$Cr_2^{III}O_3$	586.67	576.63	–	–	This work
$Cr^{VI}O_3$	588.84	579.54	–	–	This work
$LaCr^{III}O_3$	585.5	575.8	–	–	[6]
$Li_2Cr^{VI}O_4$	587.8	578.6	–	–	[5]
$LiCr^{III}O_2$	585.6	575.8	–	–	[15]
$Mn_2Ti^{IV}O_4$	–	–	462.54	456.60	
+ $MnTi^{III}O_3$	–	–	–	–	This work
			463.98	458.23	

ure 7). These shoulders appear at 578.9 eV and 585.5 eV. The presence of chromium in two different number states is the origin of the electronic conductivity in these compounds.[6]

In an attempt to study the variation in the number state of chromium caused by lithium insertion, the X-ray photoelectron spectrum of $La_{0.71}Li_{0.19}Ti_{0.69}Cr_{0.31}O_3$ before and after lithiation was recorded. In this sample the amount of inserted lithium was highest. Figure 8a shows the Cr2p spectrum of this sample. In the lithium-inserted sample (Figure 8b), the ratio between the peak areas Cr^{6+}/Cr^{3+} decreases as a result of the reduction of Cr^{6+} to Cr^{3+} with the introduction of positive charges (Li^+) in the structure.

The same study was performed for titanium (Figure 9). In both samples the titanium is present mostly as Ti^{4+}, and no change is produced in its number state during the insertion.

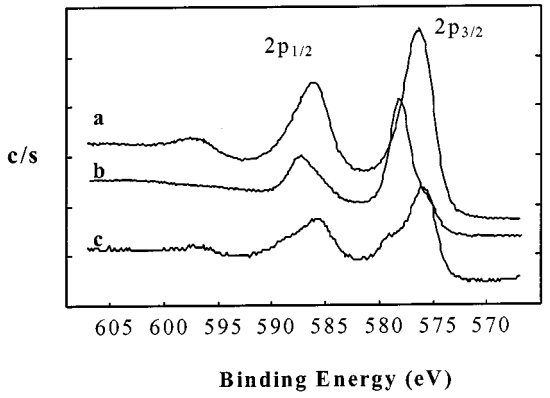

Figure 7. X-ray photoelectron spectra of Cr 2p region of: a) Cr_2O_3, b) CrO_3 and c) $La_{0.92}Li_{0.05}Ti_{0.21}Cr_{0.79}O_3$

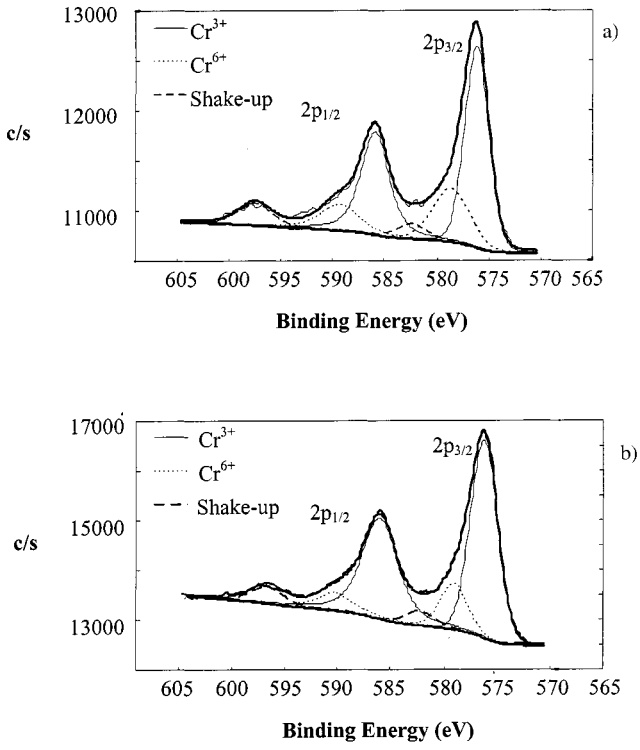

Figure 8. X-ray photoelectron spectra of Cr 2p region of: a) $La_{0.71}Li_{0.19}Ti_{0.69}Cr_{0.31}O_3$ and b) $La_{0.71}Li_{0.35}Ti_{0.69}Cr_{0.31}O_3$

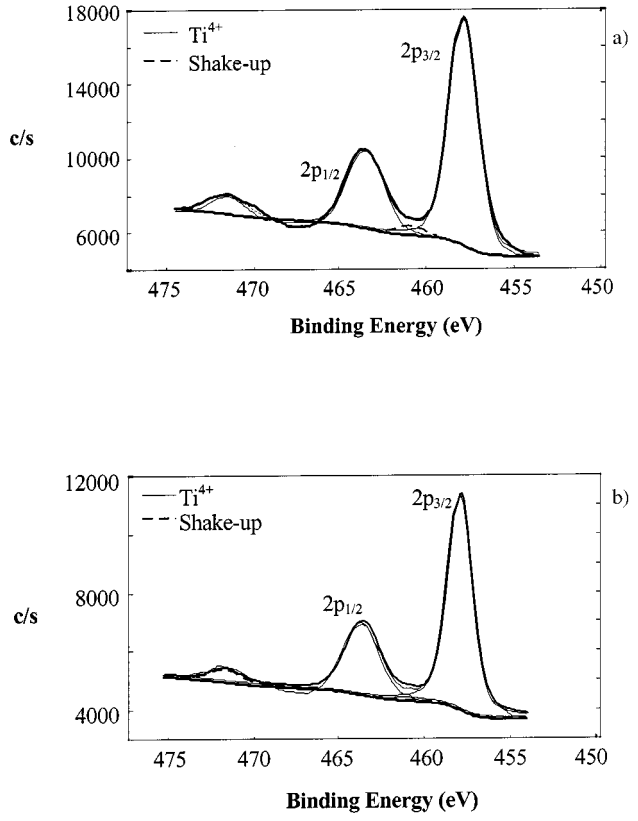

Figure 9. X-ray photoelectron spectra of Ti 2p region of: a)$La_{0.71}Li_{0.19}Ti_{0.69}Cr_{0.31}O_3$ and b) $La_{0.71}Li_{0.35}Ti_{0.69}Cr_{0.31}O_3$

Conclusion

A large range of single-phase solid solutions have been synthesized in the triangle $La_{2/3}TiO_3-LaCrO_3-La_{0.5}Li_{0.5}TiO_3$. The phase diagram in the single-phase region showed two polymorphs with a perovskite-like structure. The polymorph with the lowest chromium content has a cubic perovskite structure, and that with the highest chromium content shows an orthorhombic distortion. The cell parameters of the lithium-inserted phases show no differences with the non-lithium inserted phases. The presence of chromium in two different number states is the origin of the electronic conductivity in $La_{0.5+x+y}Li_{0.5-3x}Ti_{1-3y}Cr_{3y}O_3$.

Experimental Section

Syntheses: La_2O_3 (99.9% Fluka), TiO_2 (Aldrich 99 +%), Cr_2O_3 (>99%, Fluka) and Li_2O_3 (>99% Aldrich) were used as starting materials. La_2O_3, and TiO_2 were dried overnight at 900 °C prior to weighing. These chemicals were weighed, mixed in an agate mortar with acetone, dried and heated at 650 °C for 2 h to drive off CO_2. After grinding, samples were pressed into pellets and covered with powder of the same composition to avoid loss of lithium during the thermal treatment. The pellets were fired at 1100 °C for 8 h giving green products which were reground, repelleted, and fired at 1200 °C and at 1250 °C for 12 h, and again at 1300 °C for 4 h.

X-ray Diffraction: The crystalline phase identification and lattice parameters were obtained by powder X-ray diffraction with a Siemens D-500 diffractometer in reflection mode using Cu-K_α radiation. Lattice parameters were obtained using a silicon internal standard.

Chemical Lithium Intercalation: Chemical lithium intercalation was carried out by reacting the ground sample with *n*BuLi (1.6 M) in a hexane solution in a dried glove box filled with N_2 gas at 50 °C for 3 days with shaking. The X-ray diffraction pattern of the intercalate products was recorded after washing in hexane. After the chemical lithium intercalation, the samples were analysed by ICP, using a Jobin Ybon analyzer.

Electrochemical Lithium Intercalation: Electrochemical intercalation experiments were performed in Swagelok™ cells.[13] The positive electrode consisted of a ground powder mixture of the precursor and SuperP Carbon (kindly supplied by MMM, Belgium). Two sheets of Whattmand GF/D borosilicate glass fiber soaked with 1 M $LiPF_6$ in 1:1 EC/DMC electrolyte (Merck) were used as a separator, and the negative electrode consisted of lithium foil (0.38 mm thick). The cells were monitored with an Arbin BT2042 cycler operating in galvanostatic low current mode at 1Li/200 h.

X-ray Photoelectron Spectra: XPS spectra were recorded on a Perkin Elmer PHI 5500-ESCA SYSTEM with Al-K_α radiation (1486.6 eV). The energy calibration, including sample charging, was made against C(1s) peaks from the usual contamination. With a value of 83.8 eV for Au (4f 7/2), the energy is 284.8 eV. The pressure of the sample chamber was maintained below 10^{-9} Torr. The peaks were fitted by the Multipak computer program.[14]

Electron Probe Microanalysis: Some samples were studied by EPMA, to verify homogeneity, with a CAMECA SX50 EPMA instrument.

Acknowledgments

This study was partially sponsored by 1999GR00044 and PB98−1424−C02−02.

[1] M. A. K. L. Dissanayake, S. García-Martín, R. Saez-Puche, H. H. Sumathipala, A. R. West, *J. Mater. Chem.* **1994**, *4*, 1307−1308.
[2] M. A. K., L. Dissanayake, R. P. Gunawardane, H. H. Sumathipala, A. R. West, *Solid State Ionics* **1995**, *76*, 215−220.
[3] S. García Martín, A. D. Robertson, M. A. K. L. Dissanayake, A. R. West, *Solid State Ionics* **1995**, *76*, 309−314.
[4] J. C. Carver, G. K. Schweitzer, *J. Chem. Phys.* **1972**, *57*, 973−981.
[5] G. C. Allen, M. T. Curtis, A. J. Hooper, P. M. Tucker, *J. Chem. Soc., Dalton Trans* **1973**, 1675−1683.
[6] W. Y. Howng, R. J. Thorn, *J. Phys. Chem. Solids* **1980**, *41*, 75−81.
[7] C. Battistoni, J. L. Dormann, D. Fiorani, E. Paparazzo, S. Viticoli, *Solid State Commun.* **1981**, *39*, 581−585.
[8] I. Moreno, M. Morales, M. L. Martínez Sarrión, *J. Solid State Chem.* **1998**, *140*, 377.
[9] M. Morales, M. L. Martínez Sarrión, *J. Mater. Chem.* **1998**, *8*, 1853.
[10] M. L. Martínez Sarrión, L. Mestres,M. Morales, M. Herráiz, *J. Solid State Chem.* **2000**, 154.
[11] Y. Jin Shan, L. Chen, Y. Inaguma, M. Itoh, T. Nakamura, *J. Power Sources* **1995**, *54*, 397.

[12] F. García-Alvarado, A. Várez, E. Morán, M. A. Alario-Franco, *Phase Transitions* **1996**, *58*, 111.
[13] D. Guyomard, J. M. Tarascon, *J. Electrochem. Soc.* **1992**, *139*, 937.
[14] *Multipak for Windows 95*, Physical Electronics Inc. **1996**.
[15] I. Ikemoto, K, Ishii, S. Kinoshita, H. Kuroda, M. A. A. Franco, J. Thomas, *J. Solid State Chem.* **1976**, *17*, 425.

Received April 25, 2000
[I00158]